FATIGUE CRACK GROWTH SIMULATION OF SURFACE CRACKS UNDER ARBITRARY CRACK FACE LOADING

Xiaobin Lin

HBM (nCode) United Kingdom Limited, UK
Xiaobin.Lin@hbmncode.com

Abstract Fatigue crack growth was simulated for a surface crack subjected to arbitrary crack face loads. The simulation was based on the step-by-step integration of a proper fatigue crack growth law along the crack front, enabling complex crack shape changes to be directly predicted. The three-dimensional finite element method with the inverse square singularity near the crack tip considered was employed to calculate the stress intensity factors along the crack front, and the contact elements were also introduced into the cracked surface to avoid the possible overlapping between the crack faces. Several typical crack face loads were analysed, and the results including crack shape development, aspect ratio changes and stress intensity factor variations were given to validate the simulation technique. The results showed that the crack shape is dependent on the applied load and non-semielliptical surface crack profiles may be adopted by fatigue cracks. The simulation is particularly useful and necessary for the fatigue crack growth analysis in a residual stress field.

Keywords fatigue crack growth, stress intensity factor, surface crack, crack shape change

1. Introduction

Fatigue crack growth for surface cracks in plates has been extensively investigated both theoretically and experimentally. Surface cracks are very common in many engineering components and structures, such as pressure vessels, pipeline systems, off-shore and aircraft components *et al*. It has been widely observed from experimental investigations [1, 2] that a surface crack under fatigue loading always changes its crack front as it grows, and the shape by the fatigue crack subjected to both tension and bending loads is close to a semi-ellipse if neglecting the possible retardation of crack growth along the free surface.

Some efforts have been made to establish reasonable models to predict the fatigue crack growth of a two-dimensional surface crack, in which an experimental fatigue crack growth relation obtained from small specimen tests is employed. A typical model is that a surface crack is treated to have a semi-elliptical shape, and the change in crack aspect ratio is predicted. Newman and Raju [3] presented a two degree-of-freedom model, in which the change of crack aspect ratio is calculated by coupled integration of a Paris type of fatigue crack growth law along both crack depth and surface directions. In their model, the stress intensity factor (SIF) range at the free surface point was modified by the reducing 10% its value to consider the effect of the surface layer when the retardation of crack growth is often observed, and their own closed-form SIF equations were used.

For cracks subjected to a complex stress gradient, a method similar to those mentioned above is probably suitable if SIF solutions corresponding to such a stress distribution are available. Generally, these solutions are likely to be obtained by using a weight function method, or by superposing the SIF results for a series of polynomial stress distributions. However, this method is obviously incomplete. First, it includes a semi-elliptical shape assumption which is not adequate in some situations to define the actual shape adopted by the crack. Second, crack contact is not taken into account almost in all SIF solutions reported. This may happen if there are compressive stresses acting on the crack face. Using the SIF results obtained without considering crack contact might cause a big error in fatigue crack growth calculations. In this paper, a numerical method developed

by the author [4, 5] has been employed to simulate the fatigue crack growth of surface cracks under several typical and complex crack face loads. The method can directly predict, in a step-by-step way, the crack shape change without having to make a semi-elliptical crack shape assumption, and also take possible crack face contact into account. Various results are given to validate the numerical method for simulating fatigue crack growth with complex crack shape change.

2. Numerical simulation technique

It is usually considered reasonable to apply a fatigue crack growth law from small specimens that have a straight front to a curved crack front along which the stress intensity factor varies. The fatigue crack growth rate can then be expressed as a function of crack front position as follows

$$\frac{\mathrm{d}a(\xi)}{\mathrm{d}N} = f\left(\Delta K(\xi)\right) \tag{1}$$

where $a(\xi)$ and $\Delta K(\xi)$ are the local normal crack growth increment and the SIF range at an arbitrary crack front position, ξ, as shown in Fig.1. The crack growth increment can be written as

$$\Delta a(\xi) = \frac{f\left(\Delta K(\xi)\right)}{f\left(\Delta K_{\max}\right)} \Delta a_{\max} \tag{2}$$

where $\Delta a_{\max}$ is the maximum increment along the crack front, occurring at the point where the SIF is the largest. Fatigue cycles can then be calculated as follows

$$N_{\mathrm{i+1}} = N_{\mathrm{i}} + \frac{\Delta a_{\max}}{f\left(\Delta K_{\max}\right)} \quad (\mathrm{i} = 0,1,...) \tag{3}$$

By choosing an appropriate small value of $\Delta a_{\max}$, both the crack shape change and the corresponding number of fatigue cycles can be predicted if the SIF solutions along the crack front are available. For a Paris type fatigue crack growth law, we have

$$\Delta a(\xi) = \left(\frac{\Delta K(\xi)}{\Delta K_{\max}}\right)^m \Delta a_{\max}, \quad N_{\mathrm{i+1}} = N_{\mathrm{i}} + \frac{\Delta a_{\max}}{C\left(\Delta K_{\max}\right)^m} \quad (\mathrm{i} = 0,1,...) \tag{4}$$

The above equations have been used in the present simulation. However, it is worth indicating that a general fatigue crack growth rate equation including crack threshold and fracture toughness can be readily incorporated.

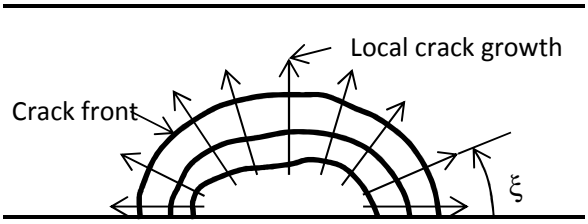

Figure 1. Illustration of fatigue crack growth of a surface crack

Stress intensity factors along the crack front were estimated by using the finite element (FE) method. The 1/4-point displacement method was used to achieve the inverse square-root stress singularity at the corner of a wedge element, and particularly possible contact between crack faces in a compressive stress field was taken into account in FE analyses. The method of estimating the SIF was detailed in [5]. Figure 2 illustrates a typical mesh created in the simulation. The mesh comprises both cracked and un-cracked blocks. Between them the “multiple point constraint” equations are applied to maintain the displacement compatibility. Both cracked and un-cracked blocks are filled with 20-node iso-parametric elements. In particular, three rings of elements are arranged surrounding the crack tip. In the simulation, the cracked block is recreated as the crack

grows whilst the un-cracked block remains unchanged.

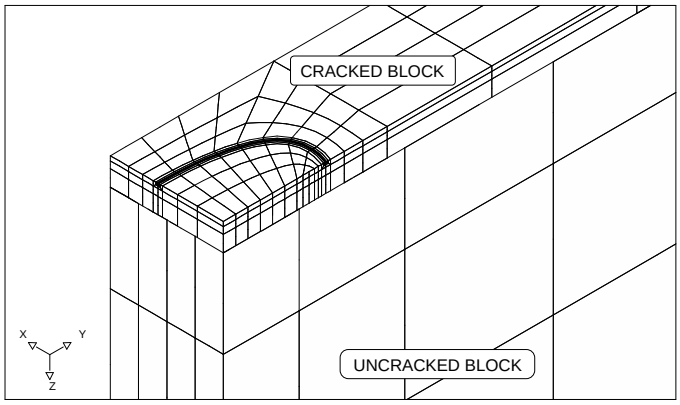

Figure 2. Type mesh configuration for stress intensity factor estimation

Local fatigue crack growth increments were calculated using the equation mentioned above, and a new crack front was established by fitting a cubic spline curve to the positions of the advanced corner nodes. Along the spline curve new corner and midside nodes were then relocated with them distanced properly. This method has been verified to be effective [6]. Automatic re-meshing of the FE model is part of the simulation technique, which makes the step-by-step simulation possible. More details can be found in [4, 6].

3. Analysis examples

Six different stress distributions varying along the plate thickness direction, as shown in Fig. 3, are considered in the present investigation. They are applied to the surface crack face in the plate as the maximum fatigue load. The minimum fatigue load is assumed to be zero.

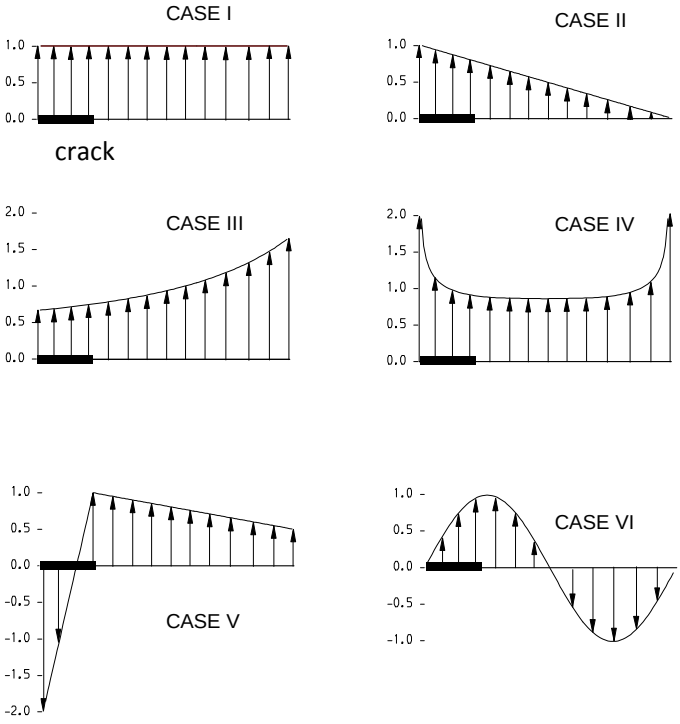

Figure 3. Crack face stresses considered in the investigation

Case I is the extensively studied loading configuration—uniform tension, i.e.

$$s(x)=1 \tag{5}$$

Case II is a combined tension and bending load that decreases linearly from unity to zero,

$$s(x)=-x/t+1 \tag{6}$$

This was selected as a representative of the linear stress variation.

Case III represents a stress variation existing on the wall of a cylindrical vessel subjected to a uniform internal pressure, which can be expressed as

$$s(x)=\frac{pR_{\mathrm{i}}^2}{R_{\mathrm{o}}^2-R_{\mathrm{i}}^2}\left(1+\frac{R_{\mathrm{o}}^2}{(R_{\mathrm{o}}-x)^2}\right) \tag{7}$$

where R_{i} and R_{o} are the inner and outer radii of the vessel, respectively; p is the internal pressure. In the simulation, the ratio of $R_{\mathrm{o}}/R_{\mathrm{i}}$ is chosen to be 2 and p to be 1 MPa. The location where x=0 corresponds to the external wall of the vessel, thus the modelled crack is similar to an external surface crack in a cylinder.

Case IV is a typical stress distribution existing in cruciform fillet welded joints [7], as shown in Fig. 5. Verreman *et al.* [7] proposed the following equations to describe the stress variation occurring at the weld toe

$$s(x)=\left(\frac{x}{t}\right)^{-\alpha}\sum_{i=0}^{4}\lambda_i\left(\frac{x}{t}\right)^i \quad 0\le x/t\le 0.5 \tag{8}$$

$$s(x)=\left(\frac{t-x}{t}\right)^{-\alpha}\sum_{i=0}^{4}\lambda_i\left(\frac{t-x}{t}\right)^i \quad 0.5\le x/t\le 1 \tag{9}$$

The above equations were obtained by fitting them to the two dimensional elastic element results. For the particular cruciform fillet joint shown in Fig. 4, the following parameters have been used: α=0, λ_0=0.414, λ_1=0.815, λ_2=-1.71, λ_3=4.16, λ_4=-3.7. High stress concentration can be found at the weld toe, which is the reason why the crack initiation is often induced there. This crack problem has been received a great deal of attention due to its importance in engineering practice.

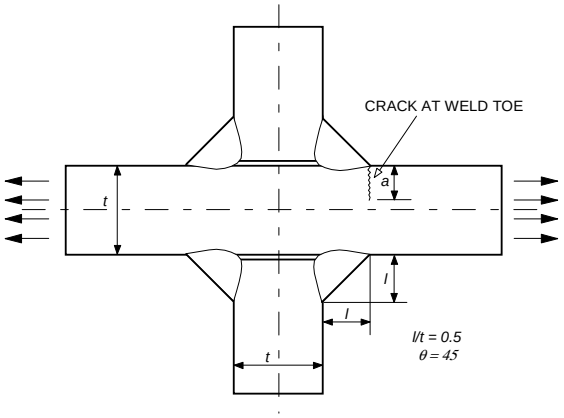

Figure 4. Cruciform fillet welded joint

Case V is used by the author to demonstrate the ability of the numerical technique to simulate the fatigue crack growth in a complex stress field containing compression. It is well known that compressive stresses are often generated on purpose to resist fatigue cracking as well as its subsequent growth. The shot peening is usually considered beneficial to delaying or even avoiding

the crack initiation from the free surface. The stress form devised here, to a certain extent, is similar to the residual stress generated by such a shot peening process. This hypothetical stress is expressed by the following equations

$$s(x)=\frac{15}{t}x-2 \qquad 0\le x\le t/5 \tag{10}$$

$$s(x)=\frac{5}{8t}x+\frac{9}{8} \qquad t/5\le x\le t \tag{11}$$

Case VI is also a hypothetical load case intended to demonstrate the capability of the numerical technique. The following is its stress distribution

$$s(x)=\sin\left(\frac{2\pi}{t}\right)x \tag{12}$$

The initial crack configuration was assumed to be a semi-circle (a/c=1) with depth ratio a/t=0.2. a, c and t are crack depth, crack surface half length, and plate thickness, respectively. The material properties employed in this investigation are: Poisson's ratio ν=0.3, Paris' fatigue crack growth relation $\mathrm{d}a/\mathrm{d}N=1.83\times10^{-13}(\Delta K)^3$

4. Results and discussion

4.1. Crack Shape Development

Figure 5 shows the fatigue crack shape development of the initially semi-circular surface crack in a plate subjected to different crack face loads. It is clear that the shape change is dependent on the load applied. The crack under uniform tension (Case I) grows with a similar growth increment along the crack front. The free surface has a slight effect on crack growth, which makes the crack advance relatively rapidly along the surface. It can be seen that the semi-elliptical shape is adequate to define the front of the propagating cracks in Fig. 5 (Case I). Crack shape change of different initial cracks for this load case has been investigated by the author [8]. It has been numerically confirmed that the widely used semi-ellipse is an adequate crack shape approximation.

The crack in Case II that has a decreasing stress value along the plate thickness propagates more rapidly in the direction of the free surface than in the direction of the plate thickness, gradually leading to a flatter crack profile. The semi-ellipse is also quite acceptable for the shape in this case, as indicated by the author [8] according to a numerical study of crack shape.

Contrary to Case II, the Case III crack extends faster at the depth than the free surface. This is due to the larger stress in the direction of crack depth. It seems that these crack profiles predicted can still be approximated with high accuracy by the semi-elliptical shape.

The stress concentration at the free surface in the Case IV load permits the crack to grow more easily along the surface compared to the crack under uniform tension fatigue (Case I). It is particularly obvious at the early stage of crack growth. The numerical crack profiles in Fig. 5 (Case IV) are basically in agreement with the experimental results obtained by Pang *et al.* [9, 10] using the beach-mark method. The growing cracks were also treated by them as those of semi-elliptical form during the crack growth calculation.

The crack face load of Case V produces an interesting result of crack shape development. The

initially semi-circular crack gradually evolves into a mushroom-shaped crack. The crack mouth is kept close and the crack, initially, is only given an opportunity of extending in a small region near the crack depth. As the cracked area becomes large, the portion of the crack front in a state of closure gradually shrinks. This is because of the increasing positive resultant stress. The maximum crack dimension can be seen to occur nearly at the *t*/4 position from the front surface, which is in accordance with the loading configuration that has the maximum tensile stress at the *t*/4 position. This phenomenon should be considered to be reasonable although no direct experimental result can be compared. The predicted crack fronts are obviously far from the semi-elliptical shape, and thus the widely used semi-elliptical crack shape assumption is not adequate for such load case. The crack shape evolution in Fig. 5 (Case V) also demonstrates that surface cracks can be effectively delayed by creating a compressive stress field near the plate surface, such as using the shot peening method.

The crack shape change illustrated in Fig. 5 for Case VI also shows that the semi-elliptical shape is not proper to be approximated to the crack fronts in this case. The lagging of crack growth along the surface can be observed, which is due to the zero stress value at the surface. The crack develops mainly in the depth direction at the early stage but the crack growth in this direction is slowed down and even stopped finally by the descending stress level as the crack extends further, see Fig. 3. The maximum crack growth is subsequently transferred to the crack front position, where the highest stress happens, i.e. at the *t*/4 position from the front surface.

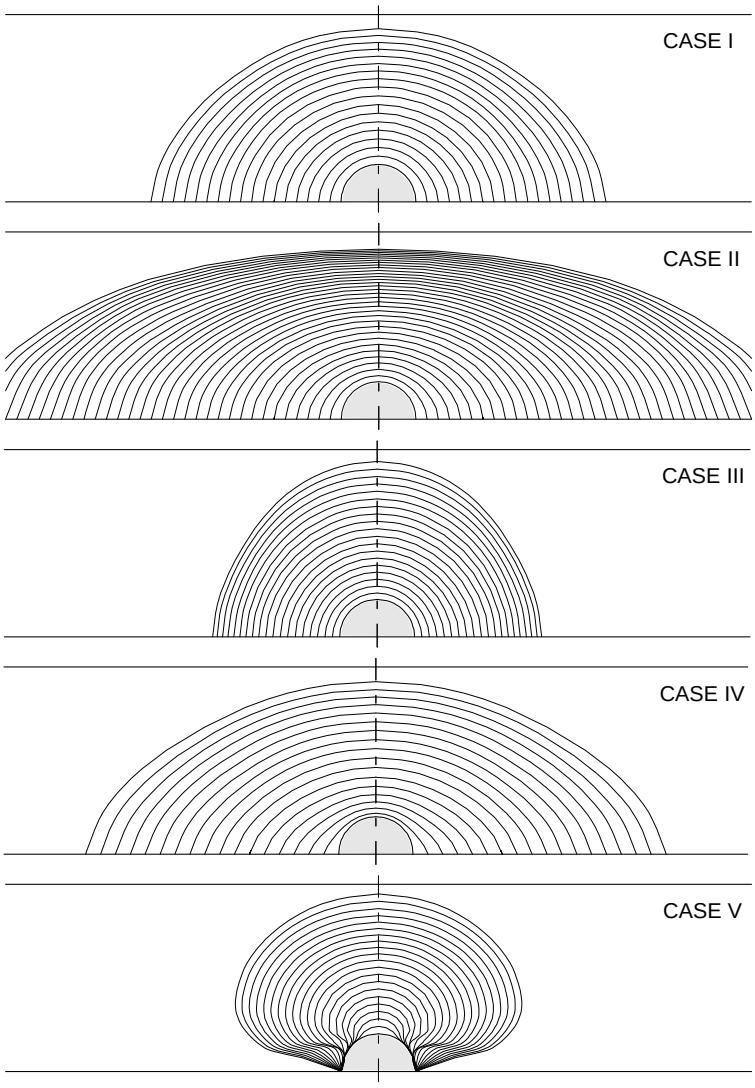

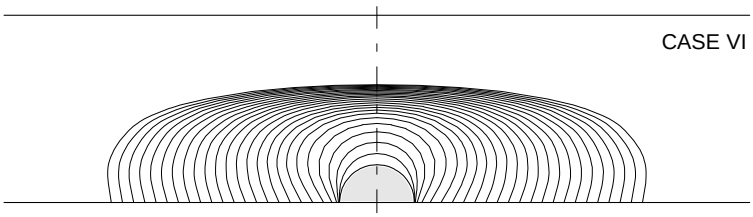

Figure 5. Fatigue shape development starting from an initially semi-circular surface crack under different crack face loads.

4.2. Aspect Ratio Change

The crack shape change is usually described quantitatively by the aspect ratio (*a*/*c*) variation with the crack depth ratio (*a*/*t*), but it should be aware that it is incomplete. The aspect ratio changes are shown in Fig. 6 for all six load cases. Clearly, the aspect ratio relation is strongly dependent on the load, as mentioned previously. The load with decreasing stress along the plate thickness makes the crack advance more difficult in this direction and eventually leads to a smaller *a*/*c* value, as seen for Cases II and IV; whilst the increasing stress along the plate thickness causes more rapid crack growth in this direction than along the surface. This can be seen in Case III. The *a*/*c* value of the Case V crack increases linearly with the *a*/*t* ratio, quickly exceeding the maximum value set in the figure. This is because no crack extension occurs along the plate surface due to the large compressive stress acting in the surface layer of the plate. However, for Case VI, the *a*/*c* value re-drops rapidly after its initial rise similar to the Case V crack, which is caused by the stress distribution with a decreasing value when the crack depth is in the region of *t*/4 and 3*t*/4. Obviously, the aspect ratio cannot give a proper description for the cracks that are not of semi-elliptical shape, like the Cases V and VI cracks.

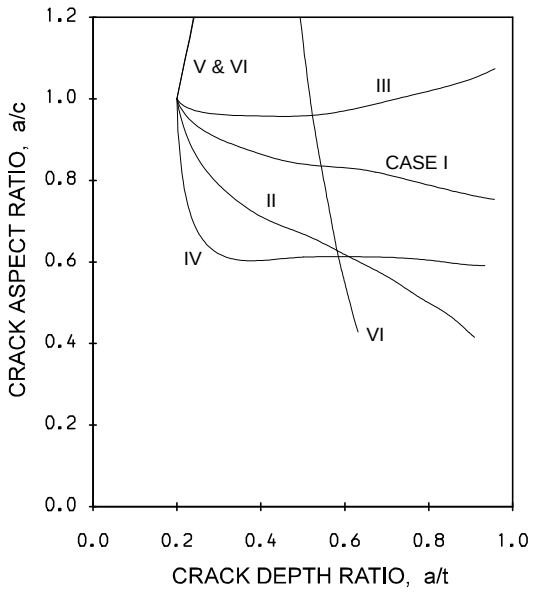

Figure 6. Aspect ratio change for surface crack under different crack face loading

Lin and Smith [8] compared the numerical results of aspect ratio predicted by the simulation technique with the experimental results for the pure tension case, i.e. Case I, and found that both the numerical and experimental results are in good agreement. This indicated that the simulation technique is effective. The numerical aspect ratio result of Case VI can be found to agree well with the experimental results of [9, 10], who carried out the fatigue test of welded joint containing a

surface crack similar to that analysed in this work for both the initial crack and joint geometries, if their result is included in Fig. 6. This further validates the present numerical technique.

4.3. Stress Intensity Factor Variation

Figure 7 shows the SIF distributions along the front of the initially circular crack (a/t=0.2) estimated by the 3D finite element method for all six load cases, where the SIF is normalised by $K_0 = \sqrt{\pi a}$. Obviously, the results vary with the applied load. The distributions along the crack front are basically uniform for Cases I, II and III, but not for Cases IV, V and VI. The SIF for Case IV shows a rapid rise at the plate surface, but that for Case VI drops when the crack front approaches the plate surface. The Case V crack gives a result that the SIF value is zero along the half crack front close to the surface, which means that the crack is in a state of partial closure under the load (Case V). It needs to be indicated that contact elements have been employed for this case. By looking at the crack face load in Fig. 3 for this case, these results are obviously reasonable.

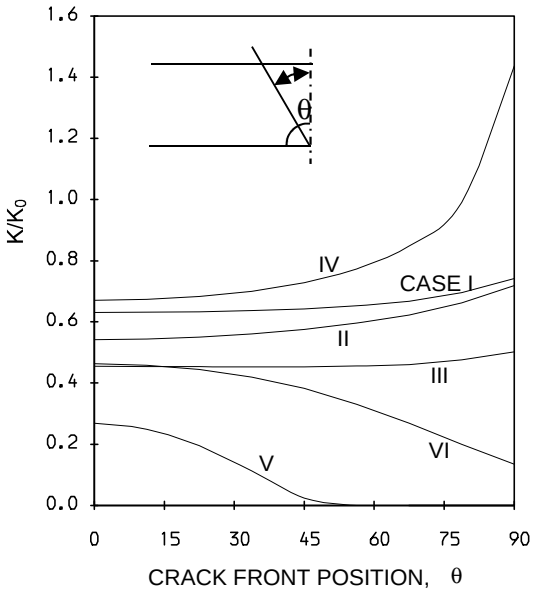

Figure 7. Stress intensity factor distributions along the initially circular crack front

The degree of the SIF non-uniformity along a crack front with crack growth is more clearly represented for all six loads in Fig. 8, where the ratio of $K_{\min}/K_{\max}$ is plotted against the crack depth ratio, a/t. It can be found that the equal K profile (the SIF value is identical around the crack front), generally, cannot be reached for non-uniform loads. Dependent on the load acting on the crack faces, complex variations exist. For Case V, rapid rise and subsequent drop in the $K_{\min}/K_{\max}$ ratio are due to the sine load, whilst for Case VI the zero variation is caused by the existence of partial closure along the crack front.

Figure 9 shows the SIF variations for all load cases at both the depth (θ=0°) and surface (θ=90°) points, where SIF has been normalized by $K_0 = \sqrt{\pi a}$. The SIF value at the depth generally increases with the crack advance except Case VI. The SIF decrease for Case VI is due to the rapid drop in stress after the crack propagates to the region of a/t<1/4. The SIF along the surface also tends to increase during crack growth, but that for Case V retains to be zero.

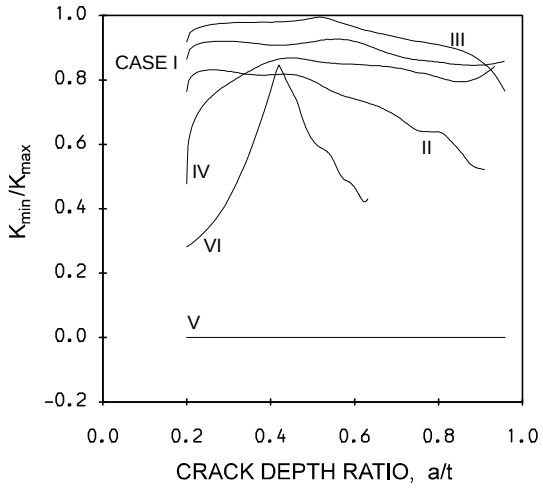

Figure 8. Change of $K_{\min}/K_{\max}$ along the crack front during crack development

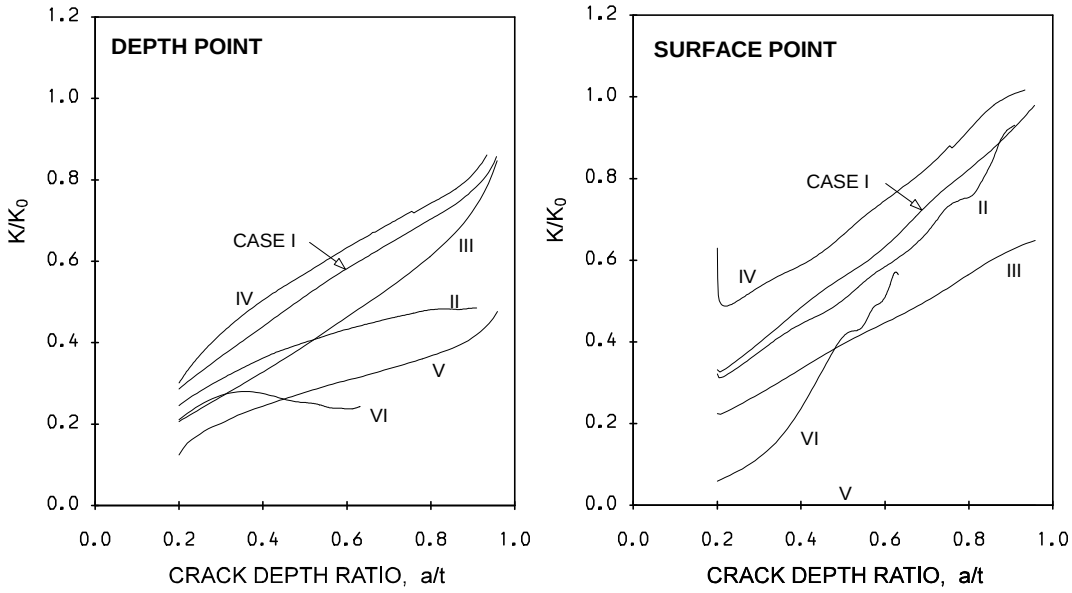

Figure 9. Stress intensity factor variations along both depth and surface points during crack growth

5. Concluding remarks

The effect of different crack face loads on fatigue crack growth of a surface crack in a plate has been investigated by using a multiple degree-of-freedom numerical method, which is based on a series of 3D FE analyses with including contact elements in cracked area and is able to directly obtain the crack shape development in a complex crack face stress field. It has been concluded that complex crack shape evolution in fatigue crack growth can be successfully predicted by the multiple degree-of-freedom numerical method. The crack profiles adopted by cracks are strongly dependent on the applied load. They might significantly deviate from the widely assumed semi-elliptical shape, although in many cases they can be approximated to such a shape. It has been also found that crack surface contact can be simulated by the contact elements introduced in the SIF calculations, so that negative SIF results can be correctly avoided.

References

[1] M.A. Mahmoud, Quantitative prediction of growth patterns of surface fatigue cracks in tension analysis. Engng Fracture Mech., 30 (1988), 735–746.
[2] M.A. Mahmoud, Growth patterns of surface fatigue cracks under cyclic bending - a quantitative analysis. Engng Fracture Mech., 31 (1989), 357–369.
[3] J.C. Jr. Newman, I.S. Raju, Analyses of surface cracks in finite plates under tension or bending loads. NASA Technical Paper 1578, 1979.
[4] X.B. Lin, R.A. Smith, Finite element modelling of fatigue growth of surface cracked plates-Part I: the numerical technique. Engng Fracture Mech., 63(5) (1999) 503–522.
[5] X.B. Lin, Estimation of stress intensity factors with considering crack surface contact. In The Thirteen European Conference on Fracture (ECF 13), San Sebastian, Spain, 6-9 September, Edited by M.R. Bache et al. 2000, pp. 1855–196.
[6] X.B. Lin, Numerical Simulation of Fatigue Crack Growth. Ph.D. thesis, The University of Sheffield, 1994.
[7] Y. Verreman, J.P. Baïlon, J. Masounav, Fatigue life prediction of welded joins—a re-assessment. Fatigue Fract. Engng Mater. Struct., 10(1), (1987) 17–36.
[8] X.B. Lin, R.A. Smith, Finite element modelling of fatigue growth of surface cracked plates-Part II: crack shape changes. Engng Fracture Mech., 63(5) (1999) 523–540.
[9] H.L.J. Pang, Analysis of weld toe profiles and weld toe cracks. Int. J. Fatigue, 15(1) (1993) 31–36.
[10] H.L.J. Pang, T.G.F. Gray, Fatigue analysis of surface cracks at fillet welded toes. Fatigue Fract. Engng Mater. Struct., 16(2) (1993) 151–164.